NIH Public Access
Author Manuscript
Glia. Author manuscript; available in PMC 2014 September 03.

Published in final edited form as:
Glia. 2008 May ; 56(7): 791–800. doi:10.1002/glia.20653.

IGF-1 Receptor-Mediated ERK/MAPK Signaling Couples Status Epilepticus to Progenitor Cell Proliferation in the Subgranular Layer of the Dentate Gyrus

YUN-SIK CHOI[1], **HEE-YEON CHO**[1], **KARI R. HOYT**[2], **JANICE R. NAEGELE**[3], and **KARL OBRIETAN**[1,*]

[1]Department of Neuroscience, Ohio State University, Columbus, Ohio

[2]Division of Pharmacology, Ohio State University, Columbus, Ohio

[3]Department of Biology, Wesleyan University, Middletown, Connecticut

Abstract

Adult progenitor cell proliferation in the subgranular zone (SGZ) of the dentate gyrus is a dynamic process that is modulated by an array of physiological process, including locomotor activity and novel environmental stimuli. In addition, pathophysiological events, such as ischemia and status epilepticus (SE), have been shown to stimulate neurogenesis. Currently, limited information is available regarding the extracellular stimuli, receptors, and downstream intracellular effectors that couple excitotoxic stimulation to progenitor cell proliferation. Here we show that pilocarpine-induced SE triggers a set of signaling events that impinge upon the p42/44 mitogen-activated protein kinase (MAPK) pathway to drive progenitor cell proliferation in the SGZ at 2-days post-SE. Increased proliferation was dependent on insulin-like growth factor-1 (IGF-1), which was localized to activated microglia near the SGZ. Using a combination of techniques, we show that IGF-1 is a CREB-regulated gene and that SE triggered CRE-dependent transcription in microglia at 2-days post-SE. Together, these data identify a potential signaling program that couples SE to progenitor cell proliferation. SE triggers CREB-dependent transcription in reactive microglia. As a CREB-target gene, IGF-1 expression is upregulated, and by 2-days post-SE, IGF-1 triggers MAPK pathway activation in progenitor cells and, in turn, an increase in progenitor cell proliferation.

Keywords

ERK; MAPK; IGF-1; progenitor cells; seizure; hippocampus; subgranular zone; pilocarpine

INTRODUCTION

Within the dentate gyrus of the hippocampus resides a bed of progenitor cells that seed the granule cell layer (GCL) throughout life. Adult-born neurons in the dentate gyrus exhibit the

© 2008 Wiley-Liss, Inc.

*Correspondence to: Karl Obrietan, Department of Neuroscience, Ohio State University, Graves Hall, Rm 4118, 333 W. 10th Ave. Columbus, OH 43210, USA. obrietan.1@osu.edu.

NIH-PA Author Manuscript
NIH-PA Author Manuscript
NIH-PA Author Manuscript

NIH-PA Author Manuscript

NIH-PA Author Manuscript

NIH-PA Author Manuscript

electrophysiological properties of granule neurons (Song et al., 2002; van Praag et al., 2002; Wang et al., 2000) and form mossy fiber projections to area CA3 (Hastings and Gould, 1999; Markakis and Gage, 1999; Stanfield and Trice, 1988), suggesting that they play an important role in activity-dependent hippocampal physiology. Indeed, external stimuli, such as exercise and hippocampal-dependent learning paradigms increase adult neural stem/progenitor cell proliferation within the subgranular zone (SGZ) (Gould et al., 1999; Olson et al., 2006) and manipulations that inhibit neurogenesis disrupt memory formation (Shors et al., 2001). These findings indicate a degree of plasticity within the pool of progenitor cells which allows the rate of proliferation to match the physiological stimulus. This plasticity extends to an array of cytotoxic insults (Parent, 2003; Picard-Riera et al., 2004). For example, both ischemia and status epilepticus (SE) induce a transient increase in the rate of SGZ neurogenesis (Liu et al., 1998; Parent et al., 1997). Although this increase in neurogenesis has been suggested to contribute to aberrant hippocampal physiology (Parent et al., 1997, 2006), the regenerative potential of adult progenitor cells make them attractive candidates for therapeutic interventions against neurodegenerative disorders. In line with this idea, the identification of the upstream neurotransmitter systems and intracellular signaling events that regulate the rate of injury-induced progenitor cell proliferation are of significant interest.

One signaling cascade that has been implicated in regulating the proliferative capacity of adult stem cells is the p42/44 mitogen-activated protein kinase (MAPK) pathway. The MAPK pathways consist of three kinases: Raf, Mek, and ERK. In the phosphorylated, and thus activated state, ERK translocates from the cytosol to the nucleus, where it regulates transcription (Chen et al., 1992). Several lines of evidence support a role for the MAPK pathway in stress-induced adult neurogenesis. First, pathophysiological stimuli, including SE and ischemia activate the MAPK pathway within the hippocampus (Choi et al., 2007; Hu et al., 2000). Second, an array of signaling molecules, including glutamate and neurotrophins stimulate both the MAPK cascade and progenitor cell proliferation and postmitotic cell differentiation (Chun et al., 2006; Deisseroth et al., 2004; Lee et al., 2002). Third, the MAPK cascade has been implicated in progenitor cell proliferation or differentiation in a number of model systems. For example, MAPK signaling has been shown to stimulate hypoxia-induced neurogenesis (Zhou and Miller, 2006; Zhou et al., 2004). These findings led us to perform a systematic examination of the potential role of the MAPK pathway in SE-induced progenitor cell proliferation in the SGZ.

Here, we propose a series of signaling events that couple SE to MAPK pathway-dependent progenitor cell proliferation in the SGZ of the dentate gyrus. The initial SE insult drives a wave of brain injury that results in microgliosis. Reactive microglia adjacent to the SGZ express the CREB-regulated gene insulin-like growth factor-1 (IGF-1). IGF-1 stimulates the MAPK pathway in progenitor cells, which, in turn, stimulates their proliferative capacity.

MATERIALS AND METHODS

Pilocarpine-Induced Status Epilepticus and Progenitor Cell Proliferation

SE was induced in male C57BL/6 mice (8 weeks of age; Harlan, Indianapolis, IN) by the intraperitoneal (i.p.) injection of pilocarpine (325 mg/kg, diluted in physiological saline,

NIH-PA Author Manuscript

NIH-PA Author Manuscript

NIH-PA Author Manuscript

Sigma, St. Louis, MO). Animals were injected (i.p.) with 1 mg/kg atropine methyl nitrate (Sigma) 30 min before injection with pilocarpine. SE was defined as a continuous motor seizure of stage 4 (rearing and falling), 5 (loss of balance, continuous rearing and falling), or stage 6 (severe tonic-clonic seizures). Allowed to run its complete course, SE persisted for 6–7 h in all mice. To label proliferating cells, 5-bromo-2′-deoxyuridine (50 mg/kg in saline, Sigma) was injected (i.p.) three times: 6, 4, and 2 h before sacrifice. Mice transgenic for the CRE-regulated β-galactosidase reporter construct were provided by Dr. Daniel R. Storm (University of Washington). All procedures were in accordance with Ohio State University animal welfare guidelines.

Immunohistochemistry and Immunofluorescence

Mice were transcardially perfused with cold phosphate-buffered saline (PBS, 10 mM, pH 7.4) followed by 4% paraformaldehyde in PBS, under ketamine/xylazine anesthesia. Brains were post-fixed in 4% paraformaldehyde for 4 h at 4°C and cryoprotected with 30% sucrose in PBS. Coronal sections (40 μm) through the dorsal hippocampus were prepared using a freezing microtome.

For immunohistochemistry, sections were washed with PBS and incubated in 0.3% hydrogen peroxide/PBS for 20 min to eliminate endogenous peroxidase activity. After several washes with PBS, sections were blocked with 10% normal goat serum in PBS, followed by overnight incubation with rabbit anti-pERK antibody (1:2,000, Cell Signaling, Danvers, MA), rabbit anti-pCREB antibody (1:2,000, Cell Signaling), rat anti-CD11b antibody (1:2,000, BioLegend, San Diego, CA), rabbit anti-c-Fos antibody (1:20,000, EMD Chemicals Inc, San Diego, CA) or mouse anti-IGF-1 antibody (1:2,000, EMD Chemicals Inc) at 4°C. Sections were then processed using the ABC staining method (Vector Labs, Burlingame, CA). Nickel-intensified DAB (Vector Labs) was used to visualize the signal. Photomicrographs were captured using a 16-bit digital camera (Micromax YHS 1300; Princeton Instruments, Trenton, NJ) mounted on a Leica DM IRB microscope (Nussloch, Germany). For BrdU staining, sections were incubated in 2XSSC/50% formamide for 2 h at 65°C, followed by incubation in 2 N HCl at 37°C for 1 h. After washing with 0.05 M borate buffer (pH 8.5) for 10 min and washing with PBS, sections were blocked with 10% normal goat serum in PBS and incubated with rat anti-BrdU antibody (1:400, Accurate Chemical, West-bury, NY) at 4°C. After washing with PBS, sections were incubated with HRP-conjugated anti-rat IgG (1:400, Jackson Immunoresearch, West Grove, PA) for 2 h at room temperature and developed with nickel-intensified DAB.

For immunofluorescence labeling, sections were blocked with 10% normal goat serum in PBS, followed by overnight incubation with mouse anti-nestin antibody (1:1,000, Millipore, Billerica, MA), rabbit anti-pERK antibody (1:1,000, Cell Signaling), rabbit anti-pCREB antibody (1:1,000, Cell Signaling), rabbit anti-c-Fos antibody (1:10,000, EMD Chemicals Inc), rabbit anti-Ki67 antibody (1:1000, Vector Labs) or rabbit anti-β-galactosidase antibody (1:50,000, Cortex Biochem, San Leandro, CA). After several washes, sections were incubated with secondary antibodies conjugated with Alexa 488, Alexa 546, Alexa 594, or Alexa 633 (1:1,000, Invitrogen, Carls-bad, CA) for 2 h at room temperature, then mounted

NIH-PA Author Manuscript

NIH-PA Author Manuscript

NIH-PA Author Manuscript

with Cytoseal (Richard-Allan Scientific, Kalamazoo, MI). Fluorescence images were captured using a Zeiss 510 Meta confocal microscope (2-μm thick optical section).

Drug Microinfusion

Mice were placed in a stereotaxic frame (David Kopf Instruments) under ketamine/xylazine anesthesia and guide cannulae (24G) were aimed at the suprapyramidal blade of dentate gyrus (stereotaxic coordinates: AP: −1.75 mm, ML: +1.00 mm, DV: −1.75 mm). Following surgery, mice were allowed to recover for 10 days. At the indicated time points, mice were restrained by hand and infused (1 μL) with U0126 (10 mM in DMSO, A.G. Scientific, San Diego, CA), AG1024 (1 mM in DMSO, EMD Chemicals Inc), MK801 (10 mM in DMSO Sigma/RBI, St. Louis, MO), or vehicle (DMSO) through an injector cannula (30G) for 2 min.

Cell Quantitation

To measure GCL/SGZ area, photomicrographs were captured at 10× magnification using a 16-bit digital camera and quantitation was performed using Meta-Morph software (Universal Imaging). The total number of BrdU-positive cells was counted bilaterally in each animal at 40–100× magnification from three dorsal hippocampal sections (AP coordinate of first, dorsal-most, section: −1.40 μm) separated by 160 μm intervals. The number of cells was given as mean ± SEM from 5–6 mice in each group. Cell counts were analyzed statistically using the nonparametric Wilcoxon rank-sum test, and significance was accepted for $P < 0.05$.

Mixed Microglial Cell Culture

Mixed microglia cultures were prepared using the method described by Saura et al. (2003) with minor modification. Briefly, mixed glial cultures were prepared from cerebral cortices of 1-day-old C57Bl/6 mice. After mincing with a razor blade, tissue was transferred to pre-warmed papain (100 U/mg, Sigma) dissociation media and incubated for 25 min at 37°C. After washing with DMEM containing 10% FBS, the tissue was triturated and cortical cells were plated at a density of 250,000 cells/mL (density of ~65,000 cells/cm^2) in a 100-mm culture dish and cultured in DMEM with 10% FBS and penicillin/streptomycin at 37°C in a humidified incubator (5% CO_2/95% air). Media was replaced every 4–5 days; confluency was attained after 10–12 days *in vitro*. Cultures were then trypsinized (0.05% trysin for 5 min, Invitrogen), and suspended. Viable cells, including microglia, were seeded in poly-D-lysine-coated 24-well plates and cultured as described above. At 3-days post-plating, 85% of cells were microglia, as assessed by double labeling with Hoecht and CD11b. This value approximates the microglial purity reported by Saura et al. (2003).

IGF-1 Induction in Cultured Microglia

Mixed microglia cultures were transfected (4 μg of DNA per well) after 3 days in culture with Lipofectamine 2000 (Invitrogen) using the manufacturer's guidelines. Cells were transfected with eGFP (500 ng/well) and either pcDNA (empty vector: 3.5 μg/well) or A-CREB (3.5 μg/well). Two days after transfection microglia were stimulated with forskolin (10 μM, Invitrogen) for 6 h. To examine IGF-1 expression in microglia, cultures were

NIH-PA Author Manuscript

NIH-PA Author Manuscript

NIH-PA Author Manuscript

initially washed with cold PBS, blocked (30 min) with 3% bovine serum albumin, and then incubated with rat anti-CD11b antibody (1:4,000, BioLegend) for 15 min at 4°C. After washing with cold PBS, cultures were incubated (30 min) with Alexa 546-conjugated anti-rat IgG (1:1,000, Invitrogen) at 4°C. Next, cultures were washed with cold PBS, and fixed (3 min) with 4% paraformaldehyde. After permeabilization with PBS containing 0.01% Triton X-100 for 1 min and blocking with 3% BSA for 30 min, cells were incubated with rabbit anti-eGFP antibody (1:8,000 University of Alberta) and mouse anti-IGF-1 antibody (1:2,000, EMD Chemicals Inc) for 1 h at RT. Finally, cultures were incubated (30 min at RT) with Alexa 488-conjugated anti-rabbit IgG and Alexa 633-conjugated anti-mouse IgG, washed and mounted with cytoseal.

RESULTS

Temporal Profile of SE-Induced Progenitor Cell Proliferation

Initially, we examined the time course of seizure-induced cell division in the SGZ of the dentate gyrus. To this end, mice (C57Bl/6) were injected with pilocarpine (325 mg/kg, i.p.). For these studies, we limited our analysis to mice that developed SE. SE was defined as continuous motor seizures (rearing and falling, loss of balance) or severe tonic-clonic seizures (Racine, 1972). SE lasted for 6–7 h, and out of the 103 mice injected with pilocarpine, SE was induced in 66% of the animals and the mortality rate was 26%. To monitor the rate of newly generated cells, mice were injected with 5-bromo-2′-deoxyuridine (BrdU, 50 mg/kg) three times at 2-h intervals and sacrificed 2 h after the last injection. Relative to saline-injected control mice, SE elicited a significant increase in the rate of cell proliferation. At 7-h post SE, the number of BrdU-positive cells nearly doubled, and by 2-days post-SE, cell division had increased by ~ fourfold relative to control levels. By 5-days post-SE the number of BrdU-labeled cells had returned to near baseline levels (Figs. 1A,B). These data are consistent with prior studies, which showed increased cell proliferation from as early as 3-h post-SE by pilocarpine (Hagihara et al., 2005; Radley and Jacobs, 2003).

SE Stimulates MAPK Pathway Activation in the Subgranular Zone

Next, we examined the potential receptors and intracellular signaling events that couple seizure activity to an increase in progenitor cell proliferation. To this end, we focused on the activation state of the MAPK pathway. This signaling pathway was the focus because prior studies have shown that SE stimulates robust activation of the MAPK pathway, and that its downstream target CREB regulates adult progenitor cell proliferation (Choi et al., 2007; Nakagawa et al., 2002; Zhu et al., 2004).

Immunohistochemical labeling for the phospho-activated form of ERK (pERK: a marker of MAPK pathway activity) revealed that SE triggered MAPK pathway activation in the dentate gyrus; induction was observed at both 15-min post-SE and 2 days after SE (Fig. 2A). Interestingly at 15 min and 2-days post-SE, distinct differences in the pERK expression pattern were observed within the dentate gyrus. At the 15 min time point, robust pERK expression was clearly detected within granule cells. However, at 2 days, pERK expression was largely limited to cells located within the SGZ. To determine whether SE stimulated MAPK pathway activation in progenitor cells, tissue was double-labeled for pERK and

NIH-PA Author Manuscript

NIH-PA Author Manuscript

NIH-PA Author Manuscript

Ki-67. High magnification microscopy of the SGZ revealed an increase in pERK expression in Ki-67-positive cells (Fig. 2B). Similarly, activated ERK was detected in nestin-positive cells of the SGZ at 2-days post-SE (Fig. 2C).

To assess whether ERK-regulated target genes were also activated, we examined the expression pattern of c-Fos. Similar to pERK, c-Fos exhibited temporally distinct expression patterns (Fig. 2A). Thus, at 4-h post-SE onset, c-Fos induction was observed in the granule cell region, whereas by 2 days, marked expression was detected specifically within nestin-positive cells of the SGZ (Figs. 2A,C). Altogether, data from Fig. 2 show that SE stimulates a MAPK signaling program in neuronal progenitor cells of the SGZ.

Regulation of the MAPK Pathway by Insulin-like Growth Factor-1 (IGF-1) in Neuronal Progenitor Cells

To elucidate the mechanism underlying SE-induced progenitor cell proliferation, we focused on the 2-days post SE time point, when maximal cell proliferation was observed. First, we examined the signaling events that couple SE to MAPK activation. Initially, we tested the role of NMDA receptor signaling. Infusion of the NMDA receptor antagonist MK801 (10 mM, 1 μL), 2 hr before sacrifice did not alter ERK activation in the SGZ (Fig. 3A), indicating that NMDA receptor activity does not drive MAPK signaling in the SGZ at 2-days post SE. To ensure that our infusion paradigm was capable of effectively inhibiting NMDA receptor activity, we tested the effects of MK801 on pERK expression in the GCL during the initial bout of SE. To this end, MK801 was infused 10 min before pilocarpine injection and mice were sacrificed 15-min post-SE onset (90–120 min after MK801 infusion). Representative data in Fig. 3B reveal that MK801 infusion effectively reduced SE-induced MAPK activation, thus supporting the efficacy of our infusion paradigm. Next, we tested candidate growth factors as potential regulators of MAPK pathway activity in progenitor cells. Our attention centered on IGF-1 since it has been shown to both regulate the MAPK cascade and increase the rate of progenitor cell proliferation in the dentate gyrus (Aberg et al., 2000, 2003; Kurihara et al., 2000). Initially, we examined the expression pattern of IGF-1 in the dentate gyrus. Under control conditions minimal IGF-1 expression was detected (Fig. 4A). However, by 2-days post-SE, marked IGF-1 expression was detected in cells near the SGZ. Double-labeling for IGF-1 and CD11b (a microglial marker) revealed reactive microglia as the source of IGF-1 (Fig. 4B). Interestingly, by 5-days post-SE, IGF-1 expression had returned to near basal levels. This decrease in expression temporally correlates with both the decrease in progenitor cell proliferation and MAPK activity at the 5-day post-SE time point. Next, we examined whether IGF-1 stimulates ERK-dependent signaling in the SGZ at 2-days post-SE. For this, the IGF-1 receptor antagonist AG1024 (3-bromo-5-t-butyl-4-hydroxy-benzylidenemalonitrile, 1 mM; Párrizas et al., 1997) was infused into the hilus, and the levels of pERK and c-Fos were examined 2 h later (Fig. 4C). Disruption of IGF-1 signaling led to a dramatic decrease in ERK activation and a more modest reduction in the level of c-Fos expression within the SGZ. The relative efficacy of AG1024 is likely a reflection of the 2-h time course of the assay. Hence, AG1024 would trigger a rapid reduction in the phosphorylation state of ERK, since it is tightly coupled to IGF-1 receptor activity. Conversely, modulation of c-Fos expression, which is dictated by

NIH-PA Author Manuscript

NIH-PA Author Manuscript

NIH-PA Author Manuscript

transcriptional, translational and post-translational processes, would likely require much more time to show the same degree of regulation.

Signaling and SE-Induced Progenitor Cell Proliferation

The findings described above led us to examine the signaling events that couple SE to progenitor cell proliferation. Given that pilocarpine-induced epileptiform activity triggers a robust increase in extracellular hippocampal glutamate (Smolders et al., 1997), we tested whether the NMDA receptor is a regulator of SE-induced progenitor cell proliferation. To this end, mice were microinfused in the hilus with the NMDA receptor antagonist MK801 (10 mM, 1 μL) 2-days post-SE. To monitor cell proliferation, BrdU was injected 1, 3, and 5 h after MK801 infusion and mice were killed 2 h after the last BrdU injection. As shown in Fig. 5, MK801 did not significantly alter the rate of cell proliferation. Next, we examined whether IGF-1 regulates progenitor cell proliferation at 2-days post-SE. To this end, mice were microinfused with AG1024 (1 mM, 1 μL). AG1024 potently repressed SE-induced progenitor cell proliferation (Figs. 5A,B). Given these results and the data in Fig. 4 showing that IGF-1 stimulates MAPK activity, we tested whether MAPK signaling drives progenitor cell proliferation. Thus, mice were microinfused with the MEK1/2 inhibitor U0126 (10 mM, 1 μL) (Figs. 5A,B). Disruption of MAPK signaling potently repressed SE-induced cell proliferation, returning it to near baseline levels. Collectively, these data indicate that IGF-1 and the MAPK pathway form a signaling cassette that couples SE to progenitor cell proliferation.

CREB/CRE-Dependent Transcription Regulates IGF-1 Expression in Microglia

Thomas et al. (1996) reported that the 5′ regulatory region of the IGF-1 gene contains a cAMP response element (CRE) and that its transcription can be regulated by CREB. These findings raise the possibility that SE drives CREB-dependent transcription, which in turn stimulates IGF-1 expression in microglia. To explore this idea, we examined the pattern of CRE-mediated gene expression in the dentate gyrus at 2-days post-SE using mice transgenic for a CRE-regulated β-galactosidase reporter construct (Impey et al., 1996). Consistent with our recent work showing that SE triggers microgliosis and induction of CRE-mediated gene expression (Lee et al., 2007), we present representative data in Fig. 6A showing robust CRE-reporter expression in CD11b-positive reactive microglia near the SGZ. Similarly, at 2-days post-SE, we detected the Ser133 phosphorylated form of CREB in the reactive microglia (Fig. 6B).

Finally, to determine whether the CREB/CRE pathway regulates IGF-1 expression, mixed microglia cultures were transfected with a dominant negative CREB (A-CREB) construct. A-CREB was generated by adding an acidic amphipathic extension to the leucine zipper domain of CREB (Ahn et al., 1998). When bound to endogenous CREB, this extension blocks binding to the cyclic AMP response element and thus represses CREB-mediated transcription. To identify transfected cells, the enhanced green fluorescent protein (eGFP) construct was co-transfected. Microglia were stimulated with forskolin (10 μM, 6 h), fixed and immunolabeled for IGF-1, eGFP, and the microglial marker CD11b. This stimulation paradigm was based on work showing that a 6-h treatment with parathyroid hormone (which activates CRE-mediated gene expression: Pearman et al., 1996) induces IGF-1 expression in

NIH-PA Author Manuscript

NIH-PA Author Manuscript

NIH-PA Author Manuscript

cultured osteoblasts (McCarthy et al., 1989). As shown in Figs. 6C,D, A-CREB led to a significant decrease in forskolin-induced IGF-1 expression. In mock-treated microglia, IGF-1 was not detected. Collectively, these data suggest that SE triggers the induction of IGF-1 via a CREB-dependent mechanism in reactive microglia, and that the release of IGF-1 drives progenitor cell proliferation in the SGZ.

DISCUSSION

The goal of this study was to begin to characterize the cellular signaling events that couple SE to progenitor cell proliferation in the SGZ. The data presented here suggest that reactive microgliosis, release of IGF-1 and subsequent activation of the MAPK in progenitor cells are key events that facilitate the proliferative capacity of SGZ progenitor cells.

SE triggers a well-characterized set of histopathological alterations in the hippocampus, including the rapid loss of pyramidal cells and hilar interneurons, reactive gliosis, and later, the sprouting of mossy fibers (Morimoto et al., 2004; Parent and Lowenstein, 2002). Along these lines, we previously reported that in mice, extensive cell loss in the hilar region was detected 6-h post-SE, and by 48-h post-SE, marked cell death in area CA1 and CA3, and microgliosis was observed throughout the hippocampus (Choi et al., 2007; Lee et al., 2007). Many of these changes are initiated by the acute release of glutamate. This excitotoxic environment also leads to an increase in cytokine levels, which, when combined with high levels of glutamate likely contributes further to SE-induced brain pathology. Within this cytotoxic environment arises a dramatic increase in the rate of cell proliferation (Dash et al., 2001; Jin et al., 2001; Liu et al., 1998; Parent et al., 1997). The reported physiological and functional ramifications of SE-induced SGZ cell proliferation are quite varied. Recently, Jakubs et al. (2006) reported that under epileptic conditions, newborn granule cells have reduced excitatory input and increased inhibitory input. Thus, these neurons could have beneficial effects by increasing the threshold for seizure propagation. Conversely, other studies have shown that adult neurogenesis can contribute to dentate pathology. For example, following SE, a subset of newborn cells migrates into hilus, mature into ectopic granule cells, and contribute to recurrent seizure generation (Parent et al., 1997; Scharfman et al., 2003; Scharfman and Hen, 2007). Likewise, McCloskey et al. (2006) reported that the ectopic hilar granule cell number is correlated with recurrent seizure frequency. Furthermore, aberrant neurogenesis following seizure activity was reported to contribute to cognitive impairment (Jessberger et al., 2007). These varied physiological effects may, in part, come from the difference in the migratory paths and resultant synaptic circuitry of the newborn granule cells. These findings raise the prospect that targeted regulation (stimulation or repression) of adult neurogenesis may attenuate brain pathology. To this end, a key issue is to identify the receptor-mediated signaling events that couple SE to adult progenitor cell proliferation.

To begin to address this issue, we examined the temporal profile of SE-induced signaling in progenitor cells. A key finding from this examination was that SE triggered robust ERK activation in the SGZ at 2-days post-SE. Given that the temporal profile of SE-induced MAPK activity overlapped with the period when robust progenitor cell division occurred, we examined whether activity-dependent MAPK signaling contributes to cell proliferation.

NIH-PA Author Manuscript

NIH-PA Author Manuscript

NIH-PA Author Manuscript

To address this issue, mice were microinfused with the MEK inhibitor U0126. Disruption of MAPK signaling abrogated SE-induced cell proliferation, indicating a central role for this pathway in activity-dependent mitosis. Interestingly, the basal level of proliferation was not affected by U0126 microinfusion, indicating that the MAPK pathway is not required for constitutive cell division. This observation is similar to a recent report by Howell et al. (2005) showing that neuropeptide Y (NPY)-mediated MAPK pathway activity blocked inducible but not the basal level of proliferation. With respect to inducible proliferation, our data are consistent with a number of recent studies implicating MAPK signaling in progenitor cell proliferation. For example, neuromodulators such as cannabinoids, opioid, NPYas well as the mood stabilizer valproate increase neurogenesis via a MAPK-dependent mechanism (Hao et al., 2004; Howell et al., 2005; Jiang et al., 2005; Persson et al., 2003; Reuda et al., 2002). Furthermore, vascular endothelial growth factor-mediated proliferation of retinal progenitor cells is also dependent on MAPK signaling (Hashimoto et al., 2006), and using a slice culture technique, MAPK signaling has been shown to stimulate hypoxia-induced neurogenesis (Zhou and Miller, 2006; Zhou et al., 2004).

The MAPK cascade is activated by diverse stimuli including neurotransmitters and growth factors. The rapid (15-min post-SE) increase in ERK activation in the dentate gyrus GCL raised the possibility that progenitor cells proliferation was directly regulated by the release of glutamate. Supporting a role for NMDA receptors, Deisseroth et al. (2004) reported that NMDA receptor activation increased progenitor cell proliferation and Chun et al. (2006) found that tetanic stimulation of the perforant pathway increased neurogenesis in an NMDA receptor-dependent manner. On the other hand, NMDA receptor antagonist injection has been shown to increase progenitor cell proliferation (Cameron et al., 1995). In addition, it was reported that proliferating cells in the adult dentate gyrus do not express detectable levels of the NMDA NR1 receptor subunit (Cameron and Gould, 1996). In the data reported here, we found that the microinfusion of MK801 did not block either SE-induced MAPK activation or proliferation in the SGZ at 2-days post-SE, suggesting that a different transmitter(s) elicited MAPK activation and proliferation. Importantly, these data do not rule out the possibility that NMDA receptor activity influences the rate of proliferation prior to 2-days post-SE, the time point examined here.

To identify alternate signaling routes, we assessed whether changes in trophic support could underlie the SE-induced increase in proliferation. To this end, we focused on IGF-1 as a potential mitogenic signal. Interest was heightened by the observation that SE triggered a robust increase in reactive microglia within the SGZ region and that these cells expressed relatively high levels of IGF-1, thus raising the possibility that microglia facilitate proliferation via the release of IGF-1. We found that the IGF-1 receptor antagonist AG1024 effectively blocked SE-induced MAPK activation and attenuated progenitor cell proliferation. These observations are consistent with recent studies indicating an instructive role for microglia in SGZ cell proliferation and neurogenesis (Aarum et al., 2003; Battista et al., 2006; Walton et al., 2006; Yan et al., 2006). With respect to IGF-1, a number of studies have shown that circulating levels of IGF-1 stimulate proliferation (Aberg et al., 2000; Trejo et al., 2001). In addition, IGF-1 overexpression promotes neurogenesis and synaptogenesis in the dentate gyrus and IGF-1 knock out mouse exhibit a reduction in granule cell numbers (Beck et al., 1995; O'Kusky et al., 2000). Furthermore, Ziv et al. (2006) reported that

NIH-PA Author Manuscript

NIH-PA Author Manuscript

NIH-PA Author Manuscript

environmental enrichment-induced neurogenesis in the hilus correlates with hilar microglial activation and IGF-1 expression. Finally, in cell culture assays, the effects of IGF-1 on hippocampal progenitor cell proliferation were shown to be mediated, in part, via the MAPK pathway (Aberg et al., 2003). These findings, coupled with work implicating other trophic factors (Battista et al., 2006; Walton et al., 2006) suggest that IGF-1 is one key regulator of SE-induced progenitor cell proliferation.

The robust induction of IGF-1 led us to examine the regulatory events that couple SE to IGF-1 expression. Promoter analysis studies have shown that IGF-1 is a CREB target gene (Thomas et al., 1996). This, combined with our recent work showing that SE triggers activation of CRE-mediated gene expression in reactive microglia (Lee et al., 2007) raised the possibility that IGF-1 expression in microglia is mediated by CREB. Using a cell culture-based approach, we showed that a dominant-negative form of CREB effectively blocked IGF-1 expression. Together, these findings are schematically outlined in Fig. 7. Thus, SE-evoked glutamate release induces rapid neuronal injury, gliosis (Rizzi et al., 2003; Borges et al., 2003; Choi et al., 2007; Lee et al., 2007), and the induction of CREB-dependent transcription in both neurons and glial populations (Lee et al., 2007). As a CREB-target gene, IGF-1 expression is upregulated, and actuates cell proliferation via a MAPK-dependent mechanism.

An understanding of the cellular signaling events that regulate both activity-dependent progenitor cell proliferation and lineage-specific cell differentiation should facilitate the development of therapeutic approaches designed to ameliorate SE-induced hippocampal pathology.

Acknowledgments

Grant sponsor: The National Institutes of Health; Grant numbers: MH62335, NS47176, NS42826; Grant sponsor: Epilepsy Foundation of America; Grant number: GRT00003412.

References

Aarum J, Sandberg K, Haeberlein SL, Persson MA. Migration and differentiation of neural precursor cells can be directed by microglia. Proc Natl Acad Sci USA. 2003; 100:15983–15988. [PubMed: 14668448]

Aberg MA, Aberg ND, Hedbacker H, Oscarsson J, Eriksson PS. Peripheral infusion of IGF-I selectively induces neurogenesis in the adult rat hippocampus. J Neurosci. 2000; 20:2896–2903. [PubMed: 10751442]

Aberg MA, Aberg ND, Palmer TD, Alborn AM, Carlsson-Skwirut C, Bang P, Rosengren LE, Olsson T, Gage FH, Eriksson PS. IGF-I has a direct proliferative effect in adult hippocampal progenitor cells. Mol Cell Neurosci. 2003; 24:23–40. [PubMed: 14550766]

Ahn S, Olive M, Aggarwal S, Krylov D, Ginty DD, Vinson C. A dominant-negative inhibitor of CREB reveals that it is a general mediator of stimulus-dependent transcription of c-fos. Mol Cell Biol. 1998; 18:967–977. [PubMed: 9447994]

Battista D, Ferrari CC, Gage FH, Pitossi FJ. Neurogenic niche modulation by activated microglia: Transforming growth factor β increases neurogenesis in the adult dentate gyrus. Eur J Neurosci. 2006; 23:83–93. [PubMed: 16420418]

Beck KD, Powell-Braxton L, Widmer HR, Valverde J, Hefti F. Igf1 gene disruption results in reduced brain size, CNS hypomyelination, and loss of hippocampal granule and striatal parvalbumin-containing neurons. Neuron. 1995; 14:717–730. [PubMed: 7718235]

NIH-PA Author Manuscript

NIH-PA Author Manuscript

NIH-PA Author Manuscript

Borges K, Gearing M, McDermott DL, Smith AB, Almonte AG, Wainer BH, Dingledine R. Neuronal and glial pathological changes during epileptogenesis in the mouse pilocarpine model. Exp Neurol. 2003; 182:21–34. [PubMed: 12821374]

Cameron HA, Gould E. Distinct populations of cells in the adult dentate gyrus undergo mitosis or apoptosis in response to adrenalectomy. J Comp Neurol. 1996; 369:56–63. [PubMed: 8723702]

Cameron HA, McEwen BS, Gould E. Regulation of adult neurogenesis by excitatory input and NMDA receptor activation in the dentate gyrus. J Neurosci. 1995; 15:4687–4692. [PubMed: 7790933]

Chen RH, Sarnecki C, Blenis J. Nuclear localization and regulation of erk-and rsk-encoded protein kinases. Mol Cell Biol. 1992; 12:915–927. [PubMed: 1545823]

Choi YS, Lin SL, Lee B, Kurup P, Cho HY, Naegele JR, Lombroso PJ, Obrietan K. Status epilepticus-induced somatostatinergic hilar interneuron degeneration is regulated by striatal enriched protein tyrosine phosphatase. J Neurosci. 2007; 27:2999–3009. [PubMed: 17360923]

Chun SK, Sun W, Park JJ, Jung MW. Enhanced proliferation of progenitor cells following long-term potentiation induction in the rat dentate gyrus. Neurobiol Learn Mem. 2006; 86:322–329. [PubMed: 16824772]

Dash PK, Mach SA, Moore AN. Enhanced neurogenesis in the rodent hippocampus following traumatic brain injury. J Neurosci Res. 2001; 63:313–319. [PubMed: 11170181]

Deisseroth K, Singla S, Toda H, Monje M, Palmer TD, Malenka RC. Excitation-neurogenesis coupling in adult neural stem/progenitor cells. Neuron. 2004; 42:535–552. [PubMed: 15157417]

Gould E, Beylin A, Tanapat P, Reeves A, Shors TJ. Learning enhances adult neurogenesis in the hippocampal formation. Nat Neurosci. 1999; 2:260–265. [PubMed: 10195219]

Hagihara H, Hara M, Tsunekawa K, Nakagawa Y, Sawada M, Nakano K. Tonic-clonic seizures induce division of neuronal progenitor cells with concomitant changes in expression of neurotrophic factors in the brain of pilocarpine-treated mice. Brain Res Mol Brain Res. 2005; 139:258–266. [PubMed: 16023256]

Hao Y, Creson T, Zhang L, Li P, Du F, Yuan P, Gould TD, Manji HK, Chen G. Mood stabilizer valproate promotes ERK pathway-dependent cortical neuronal growth and neurogenesis. J Neurosci. 2004; 24:6590–6599. [PubMed: 15269271]

Hashimoto T, Zhang XM, Chen BY, Yang XJ. VEGF activates divergent intracellular signaling components to regulate retinal progenitor cell proliferation and neuronal differentiation. Development. 2006; 133:2201–2210. [PubMed: 16672338]

Hastings NB, Gould E. Rapid extension of axons into the CA3 region by adult-generated granule cells. J Comp Neurol. 1999; 413:146–154. [PubMed: 10464376]

Howell OW, Doyle K, Goodman JH, Scharfman HE, Herzog H, Pringle A, Beck-Sickinger AG, Gray WP. Neuropeptide Y stimulates neuronal precursor proliferation in the post-natal and adult dentate gyrus. J Neurochem. 2005; 93:560–570. [PubMed: 15836615]

Hu BR, Liu CL, Park DJ. Alteration of MAP kinase pathways after transient forebrain ischemia. J Cereb Blood Flow Metab. 2000; 20:1089–1095. [PubMed: 10908042]

Impey S, Mark M, Villacres EC, Poser S, Chavkin C, Storm DR. Induction of CRE-mediated gene expression by stimuli that generate long-lasting LTP in area CA1 of the hippocampus. Neuron. 1996; 16:973–982. [PubMed: 8630255]

Jakubs K, Nanobashvili A, Bonde S, Ekdahl CT, Kokaia Z, Kokaia M, Lindvall O. Environment matters: Synaptic properties of neurons born in the epileptic adult brain develop to reduce excitability. Neuron. 2006; 52:1047–1059. [PubMed: 17178407]

Jessberger S, Nakashima K, Clemenson GD Jr, Mejia E, Mathews E, Ure K, Ogawa S, Sinton CM, Gage FH, Hsieh J. Epigenetic modulation of seizure-induced neurogenesis and cognitive decline. J Neurosci. 2007; 27:5967–5975. [PubMed: 17537967]

Jiang W, Zhang Y, Xiao L, Van Cleemput J, Ji SP, Bai G, Zhang X. Cannabinoids promote embryonic and adult hippocampus neurogenesis and produce anxiolytic-and antidepressant-like effects. J Clin Invest. 2005; 115:3104–3116. [PubMed: 16224541]

Jin K, Minami M, Lan JQ, Mao XO, Batteur S, Simon RP, Greenberg DA. Neurogenesis in dentate subgranular zone and rostral subventricular zone after focal cerebral ischemia in the rat. Proc Natl Acad Sci USA. 2001; 98:4710–4715. [PubMed: 11296300]

NIH-PA Author Manuscript

NIH-PA Author Manuscript

NIH-PA Author Manuscript

Kurihara S, Hakuno F, Takahashi S. Insulin-like growth factor-I-dependent signal transduction pathways leading to the induction of cell growth and differentiation of human neuroblastoma cell line SH-SY5Y: The roles of MAP kinase pathway and PI 3-kinase pathway. Endocr J. 2000; 47:739–751. [PubMed: 11228049]

Lee J, Duan W, Mattson MP. Evidence that brain-derived neurotrophic factor is required for basal neurogenesis and mediates, in part, the enhancement of neurogenesis by dietary restriction in the hippocampus of adult mice. J Neurochem. 2002; 82:1367–1375. [PubMed: 12354284]

Lee B, Dziema H, Lee KH, Choi YS, Obrietan K. CRE-mediated transcription and COX-2 expression in the pilocarpine model of status epilepticus. Neurobiol Dis. 2007; 25:80–91. [PubMed: 17029965]

Liu J, Solway K, Messing RO, Sharp FR. Increased neurogenesis in the dentate gyrus after transient global ischemia in gerbils. J Neurosci. 1998; 18:7768–7778. [PubMed: 9742147]

Markakis EA, Gage FH. Adult-generated neurons in the dentate gyrus send axonal projections to field CA3 and are surrounded by synaptic vesicles. J Comp Neurol. 1999; 406:449–460. [PubMed: 10205022]

McCarthy TL, Centrella M, Canalis E. Parathyroid hormone enhances the transcript and polypeptide levels of insulin-like growth factor I in osteoblast-enriched cultures from fetal rat bone. Endocrinology. 1989; 124:1247–1253. [PubMed: 2645113]

McCloskey DP, Hintz TM, Pierce JP, Scharfman HE. Stereological methods reveal the robust size and stability of ectopic hilar granule cells after pilocarpine-induced status epilepticus in the adult rat. Eur J Neurosci. 2006; 24:2203–2210. [PubMed: 17042797]

Morimoto K, Fahnestock M, Racine RJ. Kindling and status epilepticus models of epilepsy: Rewiring the brain. Prog Neurobiol. 2004; 73:1–60. [PubMed: 15193778]

Nakagawa S, Kim JE, Lee R, Malberg JE, Chen J, Steffen C, Zhang YJ, Nestler EJ, Duman RS. Regulation of neurogenesis in adult mouse hippocampus by cAMP and the cAMP response element-binding protein. J Neurosci. 2002; 22:3673–3682. [PubMed: 11978843]

O'Kusky JR, Ye P, D'Ercole AJ. Insulin-like growth factor-I promotes neurogenesis and synaptogenesis in the hippocampal dentate gyrus during postnatal development. J Neurosci. 2000; 20:8435–8442. [PubMed: 11069951]

Olson AK, Eadie BD, Ernst C, Christie BR. Environmental enrichment and voluntary exercise massively increase neurogenesis in the adult hippocampus via dissociable pathways. Hippocampus. 2006; 16:250–260. [PubMed: 16411242]

Parent JM. Injury-induced neurogenesis in the adult mammalian brain. Neuroscientist. 2003; 9:261–272. [PubMed: 12934709]

Parent JM, Elliott RC, Pleasure SJ, Barbaro NM, Lowenstein DH. Aberrant seizure-induced neurogenesis in experimental temporal lobe epilepsy. Ann Neurol. 2006; 59:81–91. [PubMed: 16261566]

Parent JM, Lowenstein DH. Seizure-induced neurogenesis: Are more new neurons good for an adult brain? Prog Brain Res. 2002; 135:121–131. [PubMed: 12143334]

Parent JM, Yu TW, Leibowitz RT, Geschwind DH, Sloviter RS, Lowenstein DH. Dentate granule cell neurogenesis is increased by seizures and contributes to aberrant network reorganization in the adult rat hippocampus. J Neurosci. 1997; 17:3727–3738. [PubMed: 9133393]

Párrizas M, Gazit A, Levitzki A, Wertheimer E, LeRoith D. Specific inhibition of insulin-like growth factor-1 and insulin receptor tyrosine kinase activity and biological function by tyrphostins. Endocrinology. 1997; 138:1427–1433. [PubMed: 9075698]

Pearman AT, Chou WY, Bergman KD, Pulumati MR, Partridge NC. Parathyroid hormone induces c-fos promoter activity in osteoblastic cells through phosphorylated cAMP response element (CRE)-binding protein binding to the major CRE. J Biol Chem. 1996; 271:25715–25721. [PubMed: 8810350]

Persson AI, Thorlin T, Bull C, Zarnegar P, Ekman R, Terenius L, Eriksson PS. Mu-and δ-opioid receptor antagonists decrease proliferation and increase neurogenesis in cultures of rat adult hippocampal progenitors. Eur J Neurosci. 2003; 17:1159–1172. [PubMed: 12670304]

NIH-PA Author Manuscript

NIH-PA Author Manuscript

NIH-PA Author Manuscript

Picard-Riera N, Nait-Oumesmar B, Baron-Van Evercooren A. Endogenous adult neural stem cells: Limits and potential to repair the injured central nervous system. J Neurosci Res. 2004; 76:223–231. [PubMed: 15048920]

Racine RJ. Modification of seizure activity by electrical stimulation. II. Motor seizure. Electroencephalogr Clin Neurophysiol. 1972; 32:281–294. [PubMed: 4110397]

Radley JJ, Jacobs BL. Pilocarpine-induced status epilepticus increases cell proliferation in the dentate gyrus of adult rats via a 5-HT1A receptor-dependent mechanism. Brain Res. 2003; 966:1–12. [PubMed: 12646302]

Reuda D, Navarro B, Martinez-Serrano A, Guzman M, Galve-Roperh I. The endocannabinoid anandamide inhibits neuronal progenitor cell differentiation through attenuation of the Rap1/B-Raf/ERK pathway. J Biol Chem. 2002; 277:46645–46650. [PubMed: 12237305]

Rizzi M, Perego C, Aliprandi M, Richichi C, Ravizza T, Colella D, Veliskova J, Moshe SL, De Simoni MG, Vezzani A. Glia activation and cytokine increase in rat hippocampus by kainic acid-induced status epilepticus during postnatal development. Neurobiol Dis. 2003; 14:494–503. [PubMed: 14678765]

Saura J, Tusell JM, Serratosa J. High-yield isolation of murine microglia by mild trypsinization. Glia. 2003; 44:183–189. [PubMed: 14603460]

Scharfman HE, Hen R. Neuroscience. Is more neurogenesis always better? Science. 2007; 315:336–338. [PubMed: 17234934]

Scharfman HE, Sollas AE, Berger RE, Goodman JH, Pierce JP. Perforant path activation of ectopic granule cells that are born after pilocarpine-induced seizures. Neuroscience. 2003; 121:1017–1029. [PubMed: 14580952]

Shors TJ, Miesegaes G, Beylin A, Zhao M, Rydel T, Gould E. Neurogenesis in the adult is involved in the formation of trace memories. Nature. 2001; 410:372–376. [PubMed: 11268214]

Smolders I, Khan GM, Manil J, Ebinger G, Michotte Y. NMDA receptor-mediated pilocarpine-induced seizures: Characterization in freely moving rats by microdialysis. Br J Pharmacol. 1997; 121:1171–1179. [PubMed: 9249254]

Song HJ, Stevens CF, Gage FH. Neural stem cells from adult hippocampus develop essential properties of functional CNS neurons. Nat Neurosci. 2002; 5:438–445. [PubMed: 11953752]

Stanfield BB, Trice JE. Evidence that granule cells generated in the dentate gyrus of adult rats extend axonal projections. Exp Brain Res. 1988; 72:399–406. [PubMed: 2465172]

Thomas MJ, Umayahara Y, Shu H, Centrella M, Rotwein P, McCarthy TL. Identification of the cAMP response element that controls transcriptional activation of the insulin-like growth factor-I gene by prostaglandin E2 in osteoblasts. J Biol Chem. 1996; 271:21835–21841. [PubMed: 8702983]

Trejo JL, Carro E, Torres-Aleman I. Circulating insulin-like growth factor I mediates exercise-induced increases in the number of new neurons in the adult hippocampus. J Neurosci. 2001; 21:1628–1634. [PubMed: 11222653]

van Praag H, Schinder AF, Christie BR, Toni N, Palmer TD, Gage FH. Functional neurogenesis in the adult hippocampus. Nature. 2002; 415:1030–1034. [PubMed: 11875571]

Walton NM, Sutter BM, Laywell ED, Levkoff LH, Kearns SM, Marshall GP, Scheffler B, Steindler DA. Microglia instruct subventricular zone neurogenesis. Glia. 2006; 54:815–825. [PubMed: 16977605]

Wang S, Scott BW, Wojtowicz JM. Heterogenous properties of dentate granule neurons in the adult rat. J Neurobiol. 2000; 42:248–257. [PubMed: 10640331]

Yan YP, Sailor KA, Vemuganti R, Dempsey RJ. Insulin-like growth factor-1 is an endogenous mediator of focal ischemia-induced neural progenitor proliferation. Eur J Neurosci. 2006; 24:45–54. [PubMed: 16882007]

Zhou L, Del Villar K, Dong Z, Miller CA. Neurogenesis response to hypoxia-induced cell death: MAP kinase signal transduction mechanisms. Brain Res. 2004; 1021:8–19. [PubMed: 15328027]

Zhou L, Miller CA. Mitogen-activated protein kinase signaling, oxygen sensors and hypoxic induction of neurogenesis. Neurodegener Dis. 2006; 3:50–55. [PubMed: 16909037]

Zhu DY, Lau L, Liu SH, Wei JS, Lu YM. Activation of cAMP-response-element-binding protein (CREB) after focal cerebral ischemia stimulates neurogenesis in the adult dentate gyrus. Proc Natl Acad Sci USA. 2004; 101:9453–9457. [PubMed: 15197280]

Ziv Y, Ron N, Butovsky O, Landa G, Sudai E, Greenberg N, Cohen H, Kipnis J, Schwartz M. Immune cells contribute to the maintenance of neurogenesis and spatial learning abilities in adulthood. Nat Neurosci. 2006; 9:268–275. [PubMed: 16415867]

NIH-PA Author Manuscript

NIH-PA Author Manuscript

NIH-PA Author Manuscript

NIH-PA Author Manuscript

NIH-PA Author Manuscript

NIH-PA Author Manuscript

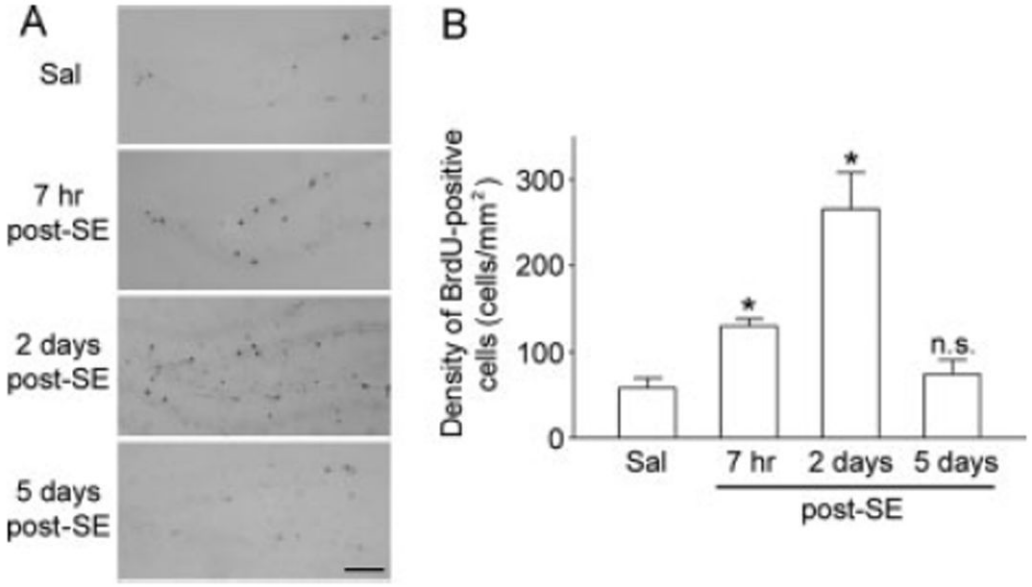

Fig. 1.

Pilocarpine-induced SE increases cell proliferation in the SGZ. **A:** Mice were injected with BrdU (three times: 2-h intervals) and perfused 2 h after the last BrdU injection. The post-SE time point is shown to the left of each panel. Scale bar = 100 μm. **B:** BrdU cell counts reveal that cell proliferation was increased at 7 h and 2-days post SE and returned near basal level by 5-days post-SE. Data were obtained from 5 to 6 mice per time point and BrdU-positive cells were counted bilaterally from three dorsal hippocampal sections per animal. The area of granule cell layer/subgranular zone was not significantly affected by pilocarpine-induced SE (0.61 ± 0.06, 0.60 ± 0.03, 0.59 ± 0.02 or 0.61 ± 0.02 mm^2 for control, 7-h, 2- or 5-days post SE, respectively). Six-10 animals were examined for each condition. Data are expressed as the mean ± SEM. *$P < 0.05$ relative to control (saline) condition.

NIH-PA Author Manuscript
NIH-PA Author Manuscript
NIH-PA Author Manuscript

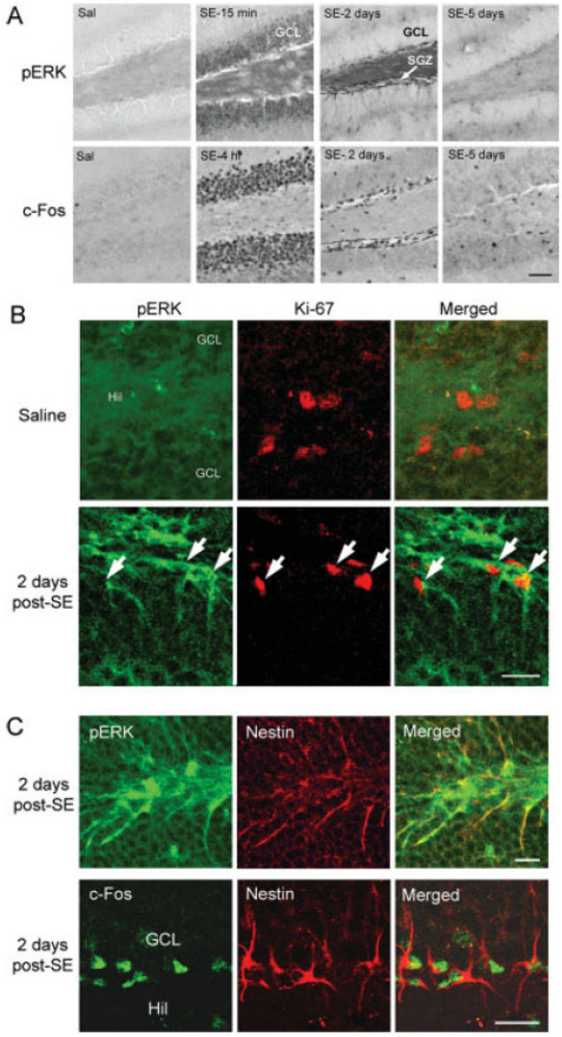

Fig. 2.

SE activates MAPK signaling in progenitor cells. **A:** Representative images of the dentate gyrus immunolabeled for pERK and c-Fos expression. Low immunoreactivity was detected under control conditions (saline injection: Sal). However, at the earlier post-SE time points (15 min and 4-h post-SE), marked pERK and c-Fos were detected in the GCL. At 2-days post-SE, pERK and c-Fos were detected in the subgranular zone (SGZ: arrow). Dashed lines approximate the SGZ boundary. Immunoreactivity returned to near baseline levels by 5-days post SE. Scale bar = 50 μm. **B:** Double-labeling revealed that ERK is activated in Ki-67 positive progenitor cells (arrows) examined 2-days post-SE. Scale bar = 20 μm. Hil: Hilus. **C:** Double-labeling revealed that pERK and c-Fos were expressed in nestin-positive progenitor cells. Data were obtained at 2-days post SE. Scale bar = 20 μm. [Color figure can be viewed in the online issue, which is available at www.interscience.wiley.com.]

NIH-PA Author Manuscript

NIH-PA Author Manuscript

NIH-PA Author Manuscript

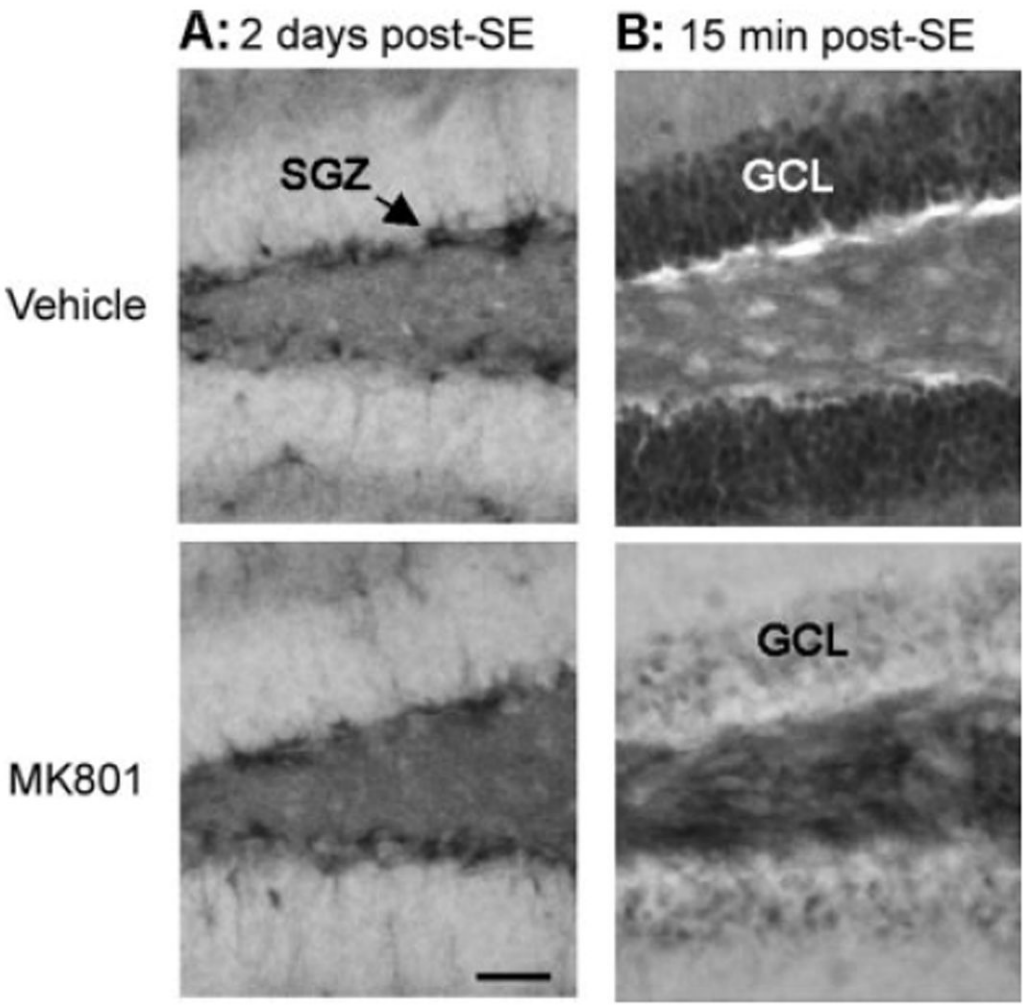

Fig. 3.

ERK activation in the SGZ. **A:** At 2 days after SE, mice were microinfused with vehicle or MK801 (10 mM) and killed 2 h later. Immunohistochemical labeling revealed that MK801 had no effect on pERK levels in the subgranular zone (SGZ: arrow). **B:** Mice were infused with MK801 10 min before pilocarpine injection and killed 15 min post-SE onset. Infusion of MK801 attenuated SE-induced MAPK pathway activation in the granule cell layer (GCL). This experiment attests to the efficacy of our microinjection technique. Scale bar = 50 μm.

NIH-PA Author Manuscript

NIH-PA Author Manuscript

NIH-PA Author Manuscript

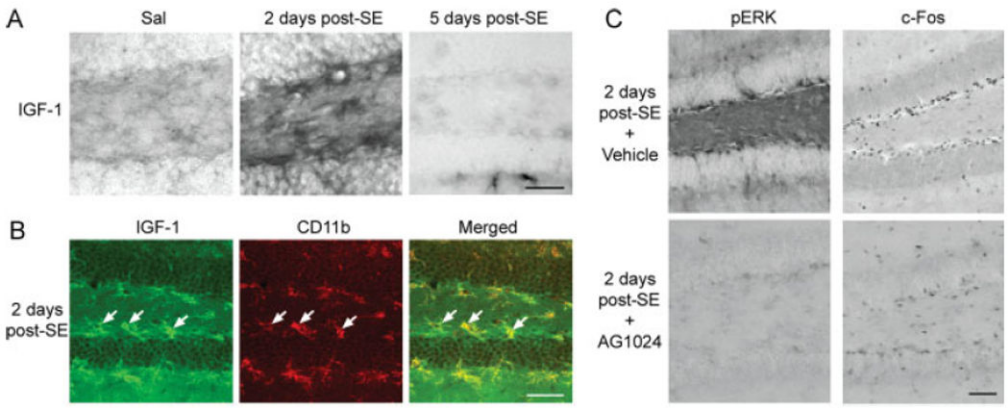

Fig. 4.

IGF-1 expression and ERK activation at 2-days post-SE. **A:** Immunohistochemical labeling revealed that IGF-1 expression was increased within the GCL border at 2-days post SE. By 5-days post-SE, IGF-1 levels returned to near control levels. Scale bar = 50 μm (**B**) Double-labeling for IGF-1 and CD11b revealed that IGF-1 was specifically expressed in microglia. Arrows denote IGF-1-positive microglia located near the SGZ. Scale bar = 50 μm. **C:** Infusion of the IGF-1 receptor antagonist, AG1024, blocked ERK activation and reduced c-Fos expression in the SGZ. AG1024 was microinfused at 2-days post-SE, and mice were sacrificed 2 h after AG1024 administration. Scale bar = 50 μm. [Color figure can be viewed in the online issue, which is available at www.interscience.wiley.com.]

NIH-PA Author Manuscript

NIH-PA Author Manuscript

NIH-PA Author Manuscript

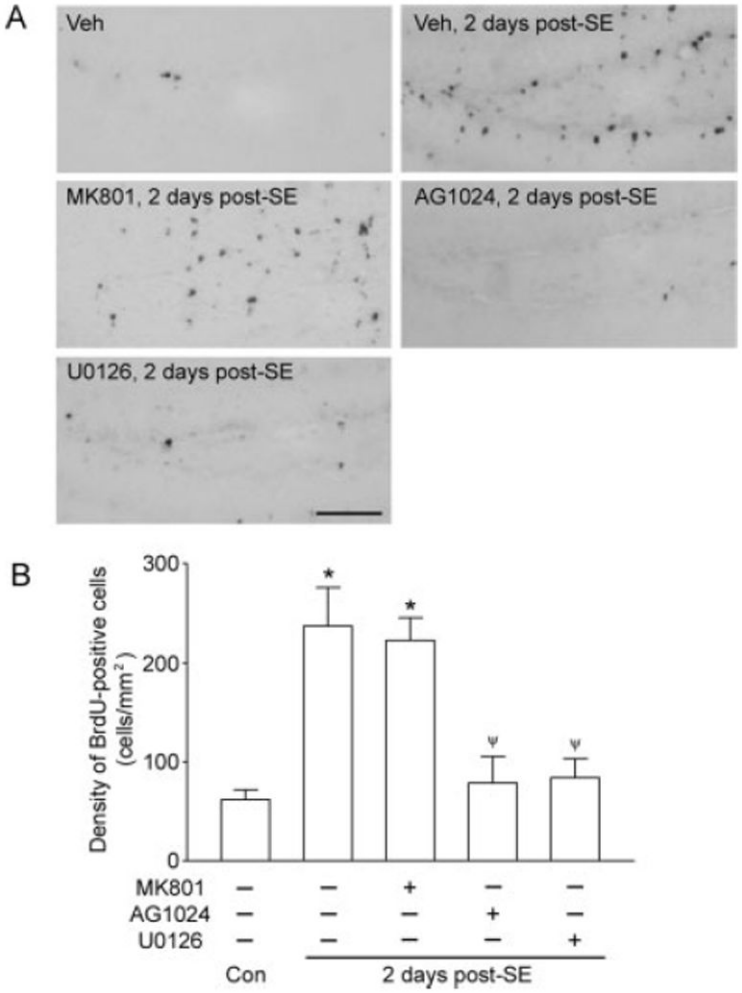

Fig. 5.

Cell proliferation, IGF-1 and the MAPK cascade. **A:** Representative images of BrdU incorporation in the dentate gyrus. BrdU was injected 1, 3, and 5 h after MK801, AG1024, U0126 or vehicle infusion. All mice were perfused 2 h after the last BrdU injection. Scale bar = 100 μm. **B:** Quantitative analysis of BrdU incorporation in the SGZ shows that SE-induced cell proliferation was inhibited by AG1024 and U0126 but not by MK801. Data were obtained from 5–6 mice for each group and expressed as the mean ± SEM. *$P < 0.01$ compared to control, $^{\Psi}P < 0.01$ compared to vehicle-injected 2-days post-SE group.

NIH-PA Author Manuscript
NIH-PA Author Manuscript
NIH-PA Author Manuscript

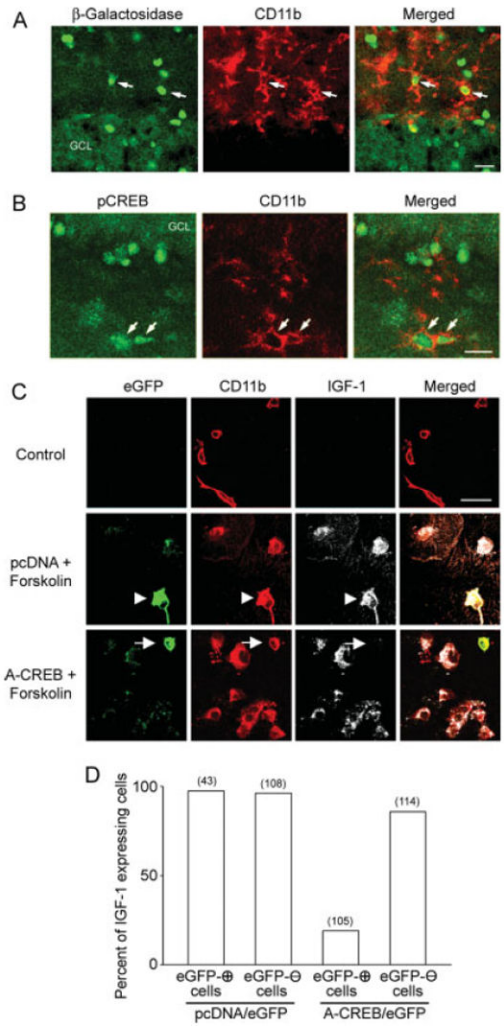

Fig. 6.

SE-induced CRE-mediated transcription and IGF-1 expression in microglia. **A,B:** Representative images from the SGZ at 2-days post-SE reveal robust expression of the transgenic CRE-regulated reporter gene, β-galatosidase, (A) and pCREB (B) in CD11b-positive microglia. Arrows identify double-labeled cells. Scale bar = 20 μm. **C:** Mixed microglia cultures were cotransfected with eGFP (transfection marker) and either dominant negative CREB (A-CREB) or pcDNA (empty vector). In untransfected and pcDNA transfected cells, forskolin (10 μM: 6-h treatment) stimulated IGF-1 expression. In A-CREB transfected cells, forskolin-induced IGF-1 expression was attenuated. Scale bar = 20 μm. Arrowhead identifies a control, empty vector, transfected cell; arrow identifies an A-CREB transfected cell. Note the lack of IGF-1 expression in the A-CREB transfected cell. To better visualize the cells, the fluorescent signal from IGF-1 immunolabeling is represented in grayscale. **D:** Analysis of forskolin-induced IGF-1 expression in A-CREB, pcDNA and untransfected cells. Unstimulated cells did not express IGF-1 (data not plotted). Numbers above each bar indicate the number of cells examined. [Color figure can be viewed in the online issue, which is available at www.interscience.wiley.com.]

NIH-PA Author Manuscript

NIH-PA Author Manuscript

NIH-PA Author Manuscript

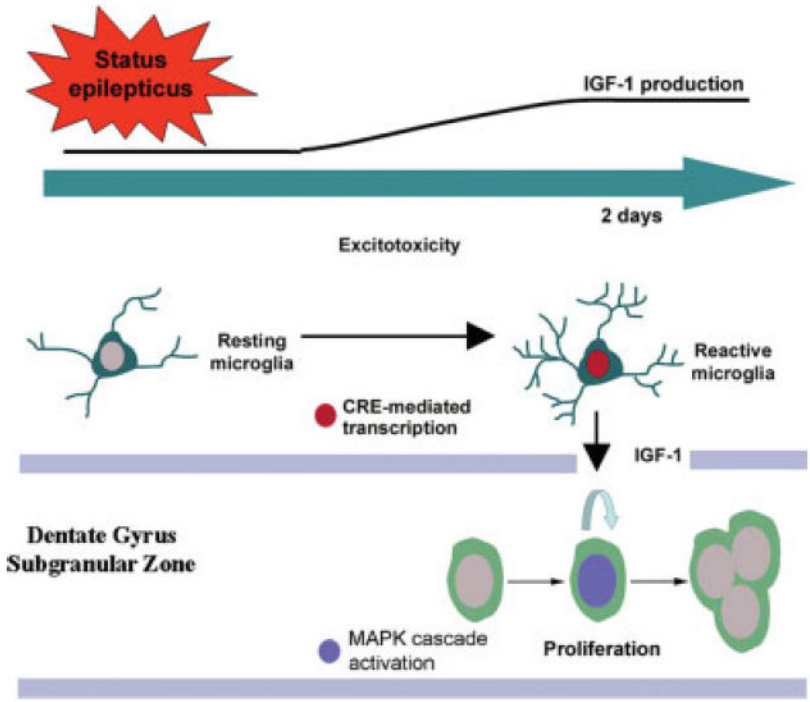

Fig. 7.

Proposed model of SE-induced progenitor proliferation: Pilocarpine-induced SE triggers glutamate release, resulting in excitotoxicity, inflammation and reactive microgliosis in the SGZ. In reactive microglia CRE-dependent transcription is activated (see Lee et al., 2007), thus leading to the expression of IGF-1. IGF-1 stimulates MAPK pathway activation, which in turn stimulates progenitor proliferation at 2-days post SE. [Color figure can be viewed in the online issue, which is available at www.interscience.wiley.com.]